Sputtering process in the presence of plasma self-organization

A. Hecimovic, N. Britun, S. Konstantinidis, and R. Snyders

Citation: Appl. Phys. Lett. **110**, 014103 (2017); doi: 10.1063/1.4973643
View online: http://dx.doi.org/10.1063/1.4973643
View Table of Contents: http://aip.scitation.org/toc/apl/110/1
Published by the American Institute of Physics

Sputtering process in the presence of plasma self-organization

A. Hecimovic,[1] N. Britun,[2] S. Konstantinidis,[2] and R. Snyders[2,3]
[1]Institute for Experimental Physics II, Ruhr-University Bochum, 44801 Bochum, Germany
[2]Chimie des Interactions Plasma-Surface (ChIPS), CIRMAP, Université de Mons, 23 Place du Parc, B-7000 Mons, Belgium
[3]Materia Nova Research Center, Parc Initialis, B-7000 Mons, Belgium

(Received 27 November 2016; accepted 22 December 2016; published online 4 January 2017)

Correlation between the plasma self-organization areas (also known as ionization zones or spokes) and the ground state/metastable atoms behavior during magnetron sputtering glow discharge is investigated. High-power impulse magnetron sputtering case is considered. For this purpose, the imaging of the ground states atomic Ti($3d^2 4s^2\ a^3F_2$), Ti^+($3d^2(^3F)4s\ a^4F_{3/2}$) and metastable Ar($3s^2 3p^5 4s\ (^3P_2)$) is performed using laser-induced fluorescence. Results indicate a correlation between the studied Ti^+ atomic density and the spoke dynamics. A qualitative model for the *spoke-assisted magnetron sputtering* is proposed, taking into account spoke formation, strong electron excitation in plasma, and other inherent phenomena of the sputtering discharge. *Published by AIP Publishing*. [http://dx.doi.org/10.1063/1.4973643]

Since 1960s, magnetron sputtering is an efficient plasma-assisted method of ejecting material from a solid cathode.[1] Under certain conditions, plasma near the cathode surface may exhibit quasi-periodic structures, observed as self-organized emission patterns acting as filaments through which the discharge current flows.[2,3] The source of filamentation is believed to be a space charge-induced field redistribution[4] created by two competing mechanisms,[5] namely, the repelling electrostatic forces between the filaments, favoring the appearance of multifilament plasma, and the charged particle diffusion, where plasma diffusion overcomes the filament repulsion, resulting in a diffuse plasma. In particular, self-organization effect has been observed in low pressure plasmas with planar magnetrons, where it is commonly referred to as ionization zones or "spokes."[6–9]

Existence of rotating instabilities in the crossed electric (**E**) and magnetic (**B**) field at low temperature plasmas has been successfully described using linearized species continuity and momentum equations[10,11] as well as by 2D Particle-in-cell Monte Carlo calculations (PIC MCC).[12,13] Fundamentally, the system evolves into the rotating structures, with azimuthally distributed zones of enhanced ionization and emission.[14,15]

Spokes exhibit different behavior depending on power applied to a planar cathode. At low power (e.g., in direct current (DC) mode), the spokes rotate along the racetrack in the $-\mathbf{E}\times\mathbf{B}$ direction[16,17] with velocities up to 2 km/s, with Ar species determining spoke dynamics.[17] At high power, realized in so-called high-power impulse magnetron sputtering (HiPIMS, where the energy up to few J is delivered in short (5–500 μs) pulses with ~1% duty cycle[18]), the spokes rotate in the $\mathbf{E}\times\mathbf{B}$ direction with velocities up to 15 km/s, with sputtered species determining the spoke dynamics.[17] Another distinctive spoke feature in HiPIMS is the unique character of their evolution from one plasma pulse to another, which is related to the fact that the information about self-organization is completely lost during the plasma-off time.

Regarding Ar-assisted sputtering, in the DC case spokes are known to be driven by Ar,[19] whereas in HiPIMS, their dynamics is defined by sputtered species.[17,20] The current understanding of spoke formation in the last case is based on creation of a potential hump within the spoke due to difference in inertia of electrons and ions resulting in cross-**B** diffusion of the plasma, away from the cathode.[14,15,21] (The experimental evidence for the potential hump is found recently).[22] The spoke rotation is governed in turn by the electrons drifting in the $\mathbf{E}\times\mathbf{B}$ direction.

The understanding of spoke dynamics achieved so far is mainly based on the experimental measurements involving optical emission spectroscopy (OES)[23–27] and electrical probes.[3,20,28] The accumulated knowledge, however, does not explain how the rotating spokes affect the distribution of *ground state* (GS) particles during the sputtering process. This letter elucidates such an influence, looking for a direct correlation between the rotating spokes and the 2D ground state density distributions of the sputtered metal atoms and singly charged ions (Ti, Ti^+ in our case), as well as Ar metastable atoms (Ar^m) in the cathode vicinity.

Laser-induced fluorescence (LIF) technique has been implemented for visualization of the mentioned atomic states in plasma.[29] A flat laser beam (70 mm wide and 2 mm thick) from a Sirah dye laser having 5 ns of the pulse duration and working at 10 Hz was located in front of the Ti cathode, parallel and at 5 mm above its surface, for the sake of excitation of plasma species in a volume of interest (VOI), as shown in Fig. 1. A fused silica cylindrical lens has been used for attaining the desirable laser beam geometry. Electron confinement region of the magnetron in our case extends up to 15 mm above the cathode surface.[30] Further details of LIF setup can be found elsewhere.[31] Such choice of the VOI is motivated by the fact that the ionization and drift processes responsible for spoke appearance and evolution mainly take place in the toroidal electron confinement region adjacent to the cathode. Discharge was ignited using Ar as a working gas at pressure of 0.67 Pa (data not shown here) and 2.7 Pa, with the following plasma parameters: pulse duration = 50 μs, repetition rate = 50 Hz, and peak current = 130 A (current waveforms are similar to one presented in Ref. 31).

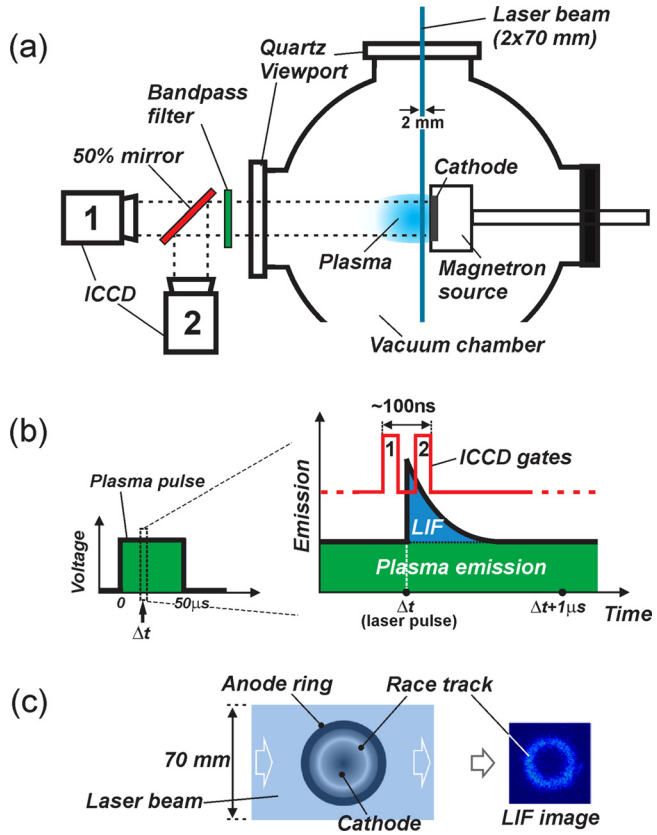

FIG. 1. Top view of the experimental setup with two ICCD detectors (a), showing the ICCD gating details relatively to the LIF signal (b), and the laser beam geometry (c).

The measurements were organized in the form of 2D LIF/OES imaging using intensified charge-coupled devices (ICCDs). Both the fluorescence and the plasma emission (referred to as OES below) were detected *simultaneously* by two ICCDs using two optical gates (≈40 ns wide) separated by a short (<20 ns) time in order to distinguish OES (ICCD1) and OES+LIF (ICCD2) signals (Fig. 1(b)). The plasma emission was filtered by optical bandpass filters (3-to-10 nm wide) corresponding to the fluorescence wavelength of the species. The LIF signal proportional to the density of the studied species has been obtained as a difference between images from the ICCD2 and ICCD1. A laser energy correction has been applied to the LIF data according to Ref. 31. Due to the non-repeatable character of spokes in HiPIMS, single-shot measurements (SSM) have been realized. The accumulative measurements (AM) were performed additionally, possessing higher signal-to-noise ratio and representing averaged dynamics of the atomic species. As a result of the ICCD gates time separation, the angular shift of the spoke patterns was measured to be ≈4°, which has been corrected in the SSM case, so the LIF and OES data for the same species in Fig. 2 can be considered corresponding to the *same* physical event. The patterns recorded for different species correspond to *different* (independent) events.

The SSM results given in Fig. 2 show the temporal evolution of 2D density distribution in the VOI (LIF signal, left columns) and the line-of-sight averaged plasma emission (OES signal, right columns) of Ti, Ti^+, and Ar^m atomic states. The delay times starting from the beginning of the plasma pulse are shown on the left. The OES signals correspond to ≈100% of Ti and Ar emission in case of Ti and Ar, and to ≈82% Ti^+/18% Ti emission in case of Ti^+ filter. The AM results are shown in Fig. 3. (The horizontal dark line seen in some cases is due to an obstacle on the way of the laser beam.)

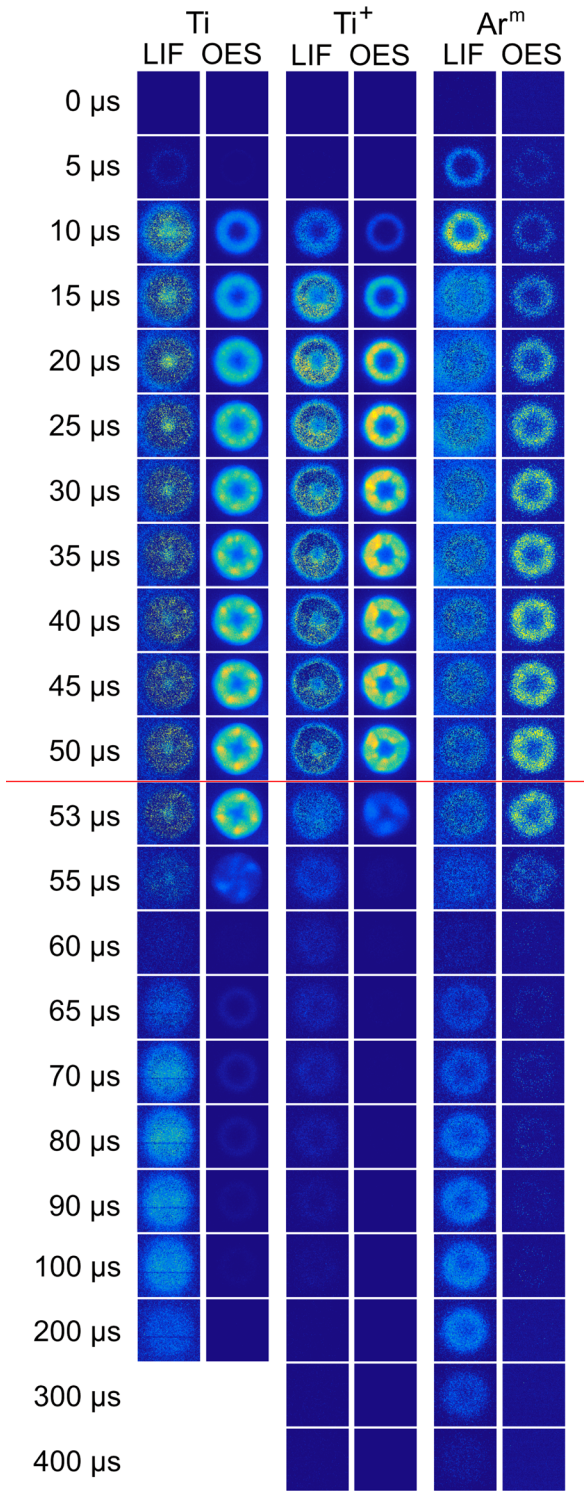

FIG. 2. Time-resolved 2D density distributions of GS Ti, Ti^+, and Ar^m above the cathode (SSM case). The left column of each species corresponds to the GS/metastable density of species (LIF signal). The right column corresponds to the plasma emission (OES signal). The red line marks the end of the pulse. Pressure 2.7 Pa. Each data column is normalized independently.

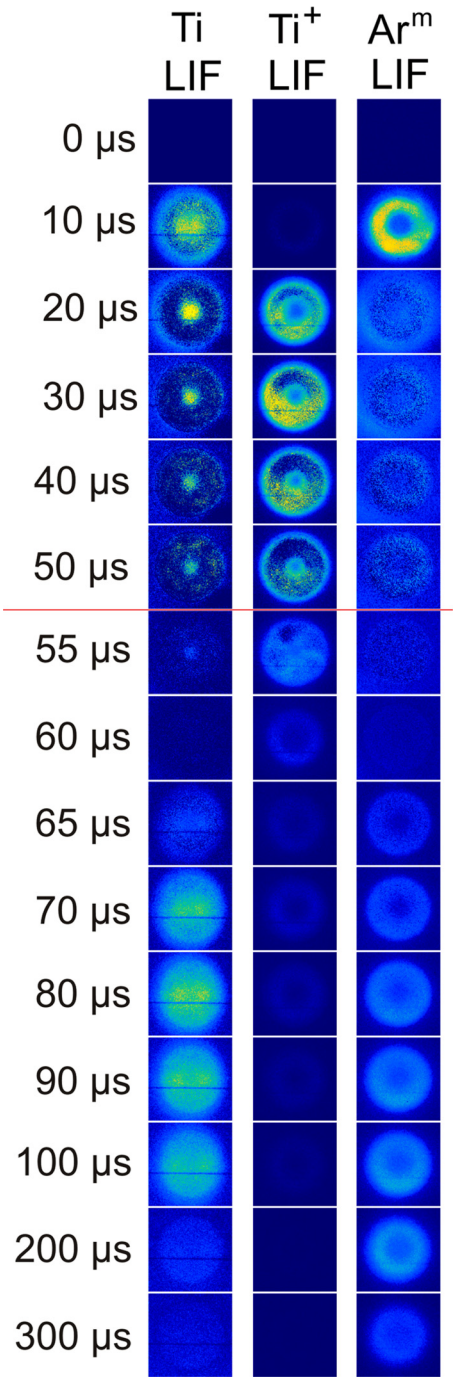

FIG. 3. Time-resolved 2D density distributions of GS Ti, Ti^+, and Ar^m above the cathode (AM case). Only LIF data are presented. The red line marks the end of the pulse. Pressure 2.7 Pa. Each data column is normalized independently.

The OES signal is present during the plasma-on time, roughly corresponding to the evolution of the discharge current, showing an increase towards the end of the pulse, Fig. 2. It appears similar for all species reflecting the level of electron excitation in the plasma.

Note that in contrast to the line-of-sight averaged OES data, LIF signal, corresponding to the species density, comes only from the VOI. At the beginning of the plasma pulse, Ar^m density shows a strong density increase at 10 μs, corresponding to the wave of electrons quickly passing through the VOI and producing Ar^m states ($E_{excit.} = 11.55$ eV).[31] Ti^+ ($E_{ioniz.} = 6.83$ eV) also shows a ring-shape GS density distribution at 10 μs, whereas GS Ti neutrals are found mainly in the center of VOI.

As plasma pulse develops, sputtering of the cathode induces Ar rarefaction and enhanced ionization of Ti. This is observed by overall reduction of Ar^m density, increase in Ti^+ density, and depletion of Ti GS density above the racetrack. Further shrinkage and final disappearance of central Ti GS maximum happens towards the end of the pulse, when it gets surrounded by a nearly zero level Ti GS density in front of the racetrack. Such evolution should be related to propagation of the sputtered Ti coming from the cathode racetrack area towards the center of the VOI,[31] which is even more clear from the AM data (Fig. 3).

In addition to ionization, the apparent density depletion is enhanced by interaction with hot plasma electrons, often leading to inversion of populations on the multiple GS energy levels.[32,33] The mentioned inversion is related to both intensive electron excitation and ionization of the ground atomic states, violating thermal (Boltzmann) population of the low energy sublevels. In HiPIMS, this effect[34] is strongly supported by the presence of highly ionized (up to Ti^{+4} (Ref. 35)) states in plasma. Gradual relaxation ($\sim$100 μs) of the level inversion happens during the off time, due to the collisions enhanced by the gas refill.[36]

Ring-shaped Ti^+ GS density distribution seen at 10 μs (Fig. 2) changes towards the discrete zero-density zones in front of the racetrack, which strongly correlates with the spoke patterns (OES data) at the end of the plasma pulse. These areas are surrounded by a non-zero density level, corresponding to the space between the spokes. At the same time, the Ar^m density depletion is barely visible, due to the high energy corresponding to this state (11.55 eV). In the afterglow, the Ti^+ GS density above the racetrack briefly increases at 55 μs, due to the gradual re-population of the depleted bottom-levels, followed by a steady decrease afterwards.

After the electron wave passing (10 μs), the Ar^m density quickly returns to its residual level (defined by excitation by cold electrons) which slowly decays till the end of the pulse, as the gas diffuses. This is followed by the gas refill after about 65 μs (Figs. 2 and 3). In general, the GS/metastable density behavior during the plasma-off time is in a very good agreement with the previous observations.[31]

The density of Ti atom and Ar^m reappears at 65 μs, and it is still visible up to $\sim$200 μs for Ti and up to $\sim$400 μs for Ar^m (Fig. 2). The observed Ti GS density increases due to the gradual re-population of the depleted bottom-levels, while for the Ar^m state, it is mainly due to the gas refill rather than depletion in this case. During this period, Ti atoms are evenly distributed above the cathode surface, while Ar^m atoms are mainly concentrated above the racetrack. Measurements at 0.67 Pa and 2.6 Pa show no influence of Ar background pressure on the timing of either Ti or Ar^m waves in the afterglow (data not shown here).

The spokes are only present during the plasma-on time, becoming pronounced after 30 μs, as the discharge current increases, exhibiting various spoke mode numbers from m = 4 to m = 6, Fig. 2. They have rather abrupt edges, pointing on a role of the secondary electrons at the end of the

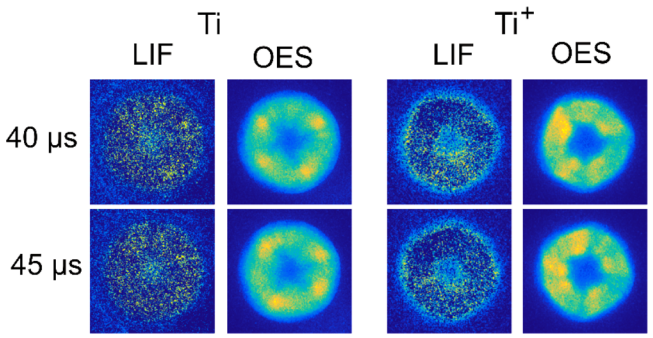

FIG. 4. The 2D density distributions of GS Ti and Ti^+ at 40 μs and 45 μs (magnified from Fig. 2).

pulse, as suggested previously.[20] Figure 4 shows 2D density distributions of GS Ti and Ti^+ at 40 μs and 45 μs, enlarged from Figure 2 for better visualization. Few distinct observations related to the spoke dynamics are as follows:

(i) *Ti neutrals*: Neglecting the sporadic Ti density variations (LIF data, Figs. 2 and 4), which are likely the artifacts of the signal subtraction or noise cancellation, the Ti GS density is generally uniformly depleted in front of the racetrack, showing no correlation with the observed spoke patterns. The observed ring-shaped minima in density for Ti GS density located around the central maximum above the racetrack represent the depletion of the Ti$(3d^24s^2\,a^3F_2)$ atomic state as described above.

(ii) *Ti ions*: Before the appearance of spokes, the non-depleted ring-shaped Ti^+ density above the racetrack is noticeable, which is followed by a reduction of Ti^+ density above the racetrack after the spokes appearance, similar to Ti neutrals. This observation is a result of the $Ti^+(3d^2(^3F)4s\,a^4F_{3/2})$ state depletion, similar to Ti neutrals, which helps in this case to visualize the LIF-OES data correlation.

(iii) *Ar metastables*: The Ar OES data barely exhibit spoke patterning at the end of the plasma pulse. The Ar^m density does not show any azimuthal inhomogeneities during this time either. During the spoke existing interval (e.g., for Ti^+), the Ar^m density is not getting fully depleted (Figs. 2 and 3, time interval between 20 and 50 μs). This is likely due to rather high Ar^m excitation threshold, as mentioned above.

Our results show that at the beginning of the discharge pulse, the spokes are diffuse and stochastic, turning into a spoke with a sharp edge as the discharge current increases. A strong reduction in Ar^m density and a strong increase in Ti^+ density indicate transition from Ar - dominated sputtering, characterized by spokes without sharp edge, to self-sputtering characterized by spokes with the sharp edge.

The spokes with sharp edge are clearly seen in Ti^+ OES signal (Fig. 2) and at the position of highest OES intensity, clearly corresponding to the minima of Ti^+ GS density. No Ti^+ depletion is observed at the racetrack edge and in the center, since the excitation, inversion, and ionization are mainly induced by the electrons captured in the toroidal confinement region of the magnetron.

OES-LIF correlation observed for Ti^+ has not been observed for Ti GS neutrals, indicating that (i) ionization and (ii) electron excitation are very high in the VOI. This implies that in this region, the non-ionized Ti exists mainly in the excited form, so no ground state (bottom level) Ti neutrals have been detected. The hypothesis about the ground state levels inversion is supported by the observation of expansion of the depleted ring-shape zone for Ti and Ti^+, which is becoming larger towards the end of the pulse. It is also in agreement with the observation of uniformly distributed Ti^+ density in the afterglow (Fig. 3), and a "wave" of Ti atoms and Ar^m atoms in the afterglow, appearing as a result of (collisional) relaxation of the electron-induced non-thermal distribution of the low-energy states. The collisional-radiative recombination from higher charged states requires three-body collisions which has negligibly small recombination rate.[4,37]

The depletion of Ti and Ti^+ inside a spoke corroborates our model of the spoke,[20] where the dynamics of the spokes in HiPIMS is defined by localised Ar gas rarefaction, and transition to self-sputtering sustained by doubly charged metal ions (M^{2+}). Within the spoke, substantial amount of these ions is required to generate secondary electrons from cathode, as they are vital for sustaining the discharge.

The data presented in this communication corroborate with spoke representation as an ionization zone mostly conducting the discharge current[3] by plasma diffusion at rates faster than Bohm diffusion[30] and driven by potential hump.[14,15] At the same time, the dynamics of the ground state density shows that the depletion of the Ti^+ ground state (bottom) level in the cathode vicinity happens at the spoke positions corresponding to maximum emission. This points out on hot electrons and higher charged states presented within a spoke, defining the correlation between its brightness and depletion of ion ground state density, whereas such correlation is absent for sputtered neutrals and Ar metastables.

The filamentary nature of current driven through a spoke is responsible for self-organized spoke patterns, due to the repulsive nature of filaments. Expectantly, due to high density of the hot electrons efficiently exciting and ionizing atomic species in the discharge, neither Ar nor sputtered Ti contributes to the spoke dynamics. Our observations may also imply that sputtering happens predominantly within a spoke following fast ionization and strong excitation of the sputtered metal atoms above the cathode, which is observed in the form of the rotative zones of depleted ground state Ti^+.

The presented results allow us to visualize a whirling plasma rotating in the $\mathbf{E} \times \mathbf{B}$ direction describing a helicoidal motion. As the plasma species are sputtered at the cathode, they get ionized in the spoke and transported in the spoke away from the cathode due to anomalous cross-**B** field diffusion.

This work was supported by the German Science Foundation (DFG), the collaborative research centre SFB-TR 87. N.B. is a post-doctoral researcher, and S.K. is a research associate of the FNRS, Belgium.

[1]E. Kay, J. Appl. Phys. **34**, 760 (1963).
[2]K. G. Müller, Phys. Rev. A **37**, 4836 (1988).

[3]P. Poolcharuansin, F. Estrin, and J. W. Bradley, J. Appl. Phys. **117**, 163304 (2015).
[4]Y. P. Raizer and M. S. Mokrov, Phys. Plasmas **20**, 101604 (2013).
[5]M. S. Benilov, Phys. Rev. E **77**, 036408 (2008).
[6]E. Martines, M. Zuin, V. Antoni, R. Cavazzana, G. Serianni, M. Spolaore, and C. Nakashima, Phys. Plasmas **11**, 1938 (2004).
[7]A. Kozyrev, N. Sochugov, K. Oskomov, A. Zakharov, and A. Odivanova, Plasma Phys. Rep. **37**, 621 (2011).
[8]A. P. Ehiasarian, A. Hecimovic, T. de los Arcos, R. New, V. Schulz-von der Gathen, M. Böke, and J. Winter, Appl. Phys. Lett. **100**, 114101 (2012).
[9]A. Anders, P. Ni, and A. Rauch, J. Appl. Phys. **111**, 053304 (2012).
[10]W. Frias, A. I. Smolyakov, I. D. Kaganovich, and Y. Raitses, Phys. Plasmas **19**, 072112 (2012).
[11]T. Ito, C. V. Young, and M. A. Cappelli, Appl. Phys. Lett. **106**, 254104 (2015).
[12]J.-P. Boeuf and B. Chaudhury, Phys. Rev. Lett. **111**, 155005 (2013).
[13]J.-P. Boeuf, Front. Phys. **2**, 295 (2014).
[14]A. Anders, M. Panjan, R. Franz, J. Andersson, and P. Ni, Appl. Phys. Lett. **103**, 144103 (2013).
[15]C. Maszl, W. Breilmann, J. Benedikt, and A. V. Keudell, J. Phys. D: Appl. Phys. **47**, 224002 (2014).
[16]Y. Yang, J. Liu, L. Liu, and A. Anders, Appl. Phys. Lett. **105**, 254101 (2014).
[17]A. Hecimovic, C. Maszl, V. Schulz-von der Gathen, M. Böke, and A. V. Keudell, Plasma Sources Sci. Technol. **25**, 035001 (2016).
[18]J. T. Gudmundsson, N. Brenning, D. Lundin, and U. Helmersson, J. Vac. Sci. Technol. A **30**, 030801 (2012).
[19]M. Panjan, S. Loquai, J. E. Klemberg-Sapieha, and L. Martinu, Plasma Sources Sci. Technol. **24**, 065010 (2015).
[20]A. Hecimovic, M. Böke, and J. Winter, J. Phys. D: Appl. Phys. **47**, 102003 (2014).
[21]A. Anders, Appl. Phys. Lett. **105**, 244104 (2014).
[22]M. Panjan and A. Anders, "Plasma potential of a moving ionization zone in DC magnetron sputtering," J. Appl. Phys. to be published.
[23]P. A. Ni, C. Hornschuch, M. Panjan, and A. Anders, Appl. Phys. Lett. **101**, 224102 (2012).
[24]J. Winter, A. Hecimovic, T. de los Arcos, M. Böke, and V. Schulz-von der Gathen, J. Phys. D: Appl. Phys. **46**, 084007 (2013).
[25]J. Andersson, P. Ni, and A. Anders, Appl. Phys. Lett. **103**, 054104 (2013).
[26]T. de los Arcos, V. Layes, Y. A. Gonzalvo, V. Schulz-von der Gathen, A. Hecimovic, and J. Winter, J. Phys. D: Appl. Phys. **46**, 335201 (2013).
[27]A. Hecimovic, V. Schulz-von der Gathen, M. Böke, A. von Keudell, and J. Winter, Plasma Sources Sci. Technol. **24**, 045005 (2015).
[28]Y. Yang, X. Zhou, J. X. Liu, and A. Anders, Appl. Phys. Lett. **108**, 034101 (2016).
[29]R. A. Stern and J. A. Johnson, Phys. Rev. Lett. **34**, 1548 (1975).
[30]A. Hecimovic, J. Phys. D: Appl. Phys. **49**, 18LT01 (2016).
[31]N. Britun, M. Palmucci, S. Konstantinidis, and R. Snyders, J. Appl. Phys. **117**, 163302 (2015).
[32]D. Ohebsian, N. Sadeghi, C. Trassy, and J. M. Mermet, Opt. Commun. **32**, 81 (1980).
[33]S. Konstantinidis, A. Ricard, M. Ganciu, J. P. Dauchot, C. Ranea, and M. Hecq, J. Appl. Phys. **95**, 2900 (2004).
[34]N. Britun, M. Palmucci, S. Konstantinidis, and R. Snyders, J. Appl. Phys. **117**, 163303 (2015).
[35]J. Andersson, A. P. Ehiasarian, and A. Anders, Appl. Phys. Lett. **93**, 071504 (2008).
[36]N. Britun, M. Palmucci, and R. Snyders, Appl. Phys. Lett. **99**, 131504 (2011).
[37]J. Stevefelt, J. Boulmer, and J.-F. Delpech, Phys. Rev. A **12**, 1246 (1975).